International Journal of Nanomedicine Dovepress

Open Access Full Text Article ORIGINAL RESEARCH

Harnessing the Power of *Saussurea obvallata* Zinc Oxide Nanoparticles for Accelerated Wound Healing and Antimicrobial Action

Adel Moalwi[1], Keerti Naik[2], Uday M Muddapur[2], Bader Aldoah[1], Hajar Hassan AlWadai[1], Abdulrahman Manaa Alamri[1], Saeed A Alsareii[1], Mater H Mahnashi[3], Ibrahim Ahmed Shaikh[4], Aejaz Abdullatif Khan[5], Sunil S More[6]

[1]Department of Surgery, College of Medicine, Najran University, Najran, Saudi Arabia; [2]Department of Biotechnology, KLE Technological University, BVB Campus, Hubballi, Karnataka, India; [3]Department of Pharmaceutical Chemistry, College of Pharmacy, King Khalid University, Abha, Saudi Arabia; [4]Department of Pharmacology, College of Pharmacy, Najran University, Najran, Saudi Arabia; [5]Department of General Science, Ibn Sina National College for Medical Studies, Jeddah, Saudi Arabia; [6]School of Basic and Applied Sciences, Dayananda Sagar University, Bangalore, Karnataka, India

Correspondence: Uday M Muddapur; Mater H Mahnashi, Email muddapur@kletech.ac.in; matermaha@gmail.com

Introduction: Zinc oxide nanoparticles (ZnONPs) have been the subject of substantial research by virtue of their utility across extensive downstream applications. Moreover, the ZnONPs are inexpensive, reliable, and easy to produce. Green synthesis employing biological systems, particularly plant extracts, has arisen as a subject of study in nanotechnology and is gaining importance due to its multiple applications in biology, chemistry, physics, and medicine.

Methods: Aqueous extract of *S. obvallata* was prepared and ZnONPs were synthesised using zinc acetate as a substrate. UV-Vis spectrophotometric measurement confirmed the production of ZnONPs. The ZnONPs were characterized by employing SEM, EDS, XRD, and FTIR. The ZnONPs were screened for its antimicrobial and wound healing potential.

Results: The peak of absorbance for UV-Vis was observed at 370 nm. The average dimension of the particles was found to be 22.58 nm. The antibacterial activity of ZnONPs was efficient in countering a broad spectrum of bacteria and the fungi *C. albicans*. The results of in vitro and in vivo wound healing assays indicate that the ZnONPs possess potent wound healing potential. In the cell migration assay, the percentage of wound closure was observed to be 84.70% ($p < 0.001$) for ZnONPs compared to the untreated group (8.12%). In the excision wound healing rat model, the animals treated with ZnONPs and Povidone-Iodine showed a significant ($p < 0.01$) wound contraction in comparison to the untreated animals.

Discussion: The ZnONPs promoted wound healing processes and showed promise as a therapeutic agent. However, further research is needed to understand the mechanisms of action and evaluate the long-term safety and effectiveness of ZnONPs in wound healing applications. By using renewable biological materials, the green synthesis of ZnONPs minimizes the need for synthetic reagents and lowers the total carbon footprint related to the production of nanoparticles.

Keywords: green synthesis, wound healing, zinc oxide NPs, *Saussurea obvallata*, antimicrobial

Introduction

Nanoparticles (NPs) are extremely small particles with sizes measured in the nanometer scale, usually between 1 and 100 nm. They can be made from a variety of materials, including metals, metal oxides, polymers, or ceramics. The 1980s and 1990s saw the emergence of the contemporary field of nanotechnology. The creation of methods like atomic force microscopy and electron microscopy, which enabled researchers to visualize and work with materials at the nanoscale, was one of the major advancements. Compared to conventional methods, nanotechnology-based therapeutic approaches target molecular and cellular processes with more safety, efficacy, and specificity.[1,2] Because of its small size, NPs frequently display distinct physical, chemical, and biological characteristics that differ from bigger materials with the same composition. These properties make NPs highly versatile and enable their application in a wide range of fields,

Received: 4 August 2024
Accepted: 26 November 2024
Published: 5 December 2024

including medicine, cosmetics, electronics, energy, environmental remediation, pharmaceuticals and many more.[3] These NPs are intriguing because their atoms are predominantly located near the surface, leading to significantly different physical and chemical properties, reactivity, and atomic arrangements compared to bulk materials.[4] The antibacterial characteristics of NPs have led to them being called as "nano antibiotics".[5] NPs are used in several consumer products, including those in the chemical, food, feed, health, and cosmetics sectors.[6,7]

There are several techniques that can be employed to synthesize NPs. The utilization of biological systems, particularly plant extracts, for green synthesis, has gained popularity in nanotechnology.[8] Green synthesis of nanoparticles offers several advantages: it is eco-friendly, utilizing non-toxic and biodegradable materials that reduce environmental impact. This method is cost-effective due to the use of readily available biological resources and typically requires mild reaction conditions, minimizing energy consumption. The resulting nanoparticles are often biocompatible, making them suitable for biomedical applications. Additionally, green synthesis can produce diverse morphologies with unique shapes and sizes, enhancing functionality while ensuring reduced toxicity from harmful chemicals. The simplicity of the process allows for easy scalability, promoting sustainability through renewable resources. Biologically synthesized nanoparticles also exhibit enhanced stability and potential for functionalization due to natural capping agents.

Zinc oxide nanoparticles (ZnONPs) have garnered significant attention due to their diverse range of potential applications across various fields.[9] According to Kalpana et al.[10] ZnONPs are economical, safe, and easy to produce. The chemical and physical properties of ZnONPs can be easily modified by using different synthesis methods, precursors, or materials.[11] These nanoparticles exhibit notable optical, electrical, and photocatalytic properties.[12] Their strong UV-absorption and non-toxic nature make ZnONPs ideal for biomedical applications. In addition, ZnONPs have a significant degree of innate resistance to microorganisms.[13] Because of these properties, ZnONPs are extensively employed in several biological applications, like drug administration, gene transfer, labelling and sensing in living organisms, and nanomedicine for diabetic wound healing.[11–14] A schematic presentation of the synthesis, characterization and biological applications has been depicted in Figure 1.

Zinc oxide is currently listed as generally recognized as safe by the US Food and Drug Administration and used as a food additive, given that zinc is an essential trace element. Zinc oxide has the potential to be used as multi-purpose nanocarrier to help with the transport and release of medications due to its solubility in an acidic environment. ZnONPs have been shown to be useful in a wide range of contexts by numerous studies, such as photocatalysis,[15] antimicrobials,[16,17] and energy cells.[18] ZnONPs generated by green synthesis display unique physical and chemical properties and are used in a variety of biological processes, such as wound healing, immunity, infection control, diabetes treatment, antifungal activities, regeneration of tissues, coatings for implants, bio-imaging, wound healing, and the development of novel anticancer medications.[19–21] A popular natural product with strong flavonoid content is *Prunus serrulata* leaves. In a previous study, the flavonoids extracted from *Prunus serrulata* were used as capping and reducing agents for ZnONPs,[22] similarly, hydrogels containing different bioactive compounds have been incorporated to promote skin wound healing.[23,24]

Saussurea obvallata (*S. obvallata*), is a flowering plant species that bears the name Brahma kamala in honor of the Hindu god of creation.[25] The Himalayan area of India has a wide variety of flora, including several endemic and rare species. Brahma kamala is considered the 'king of Himalayan flowers'. *S. obvallata* can be found in the Uttarakhand districts of Kedarnath, Hemkund Sahib, and Tungnath and is also seen in Nepal, Bhutan, and Tibet.[21] *S. obvallata* is a celestial flower that only blooms for one night each year, generally in the late summer or early autumn. It is a herb that is hermaphrodite and grows to a length of between 5 and 10 cm (Figure 2).

S. obvallata is recognized for its medicinal properties and used in the treatment of fever. Various parts of the plant, including rhizomes, flowers, and leaves, are utilized for therapeutic purposes.[26] The rhizomes are specifically noted for their antibacterial and wound healing properties and are employed in the treatment of cuts and bruises.[27] Additionally, the consumption of flower extracts has been shown to stimulate insulin production from the pancreas. *S. obvallata*, is effective in alleviating symptoms associated with asthma, bronchitis, cough, and colds, and it aids in the clearance of mucus from the respiratory tract.[28] These findings support the traditional use of *S. obvallata* in herbal medicine and highlight its potential therapeutic applications. Floral extracts contain a wide range of phytochemicals, including polyphenols, flavonoids, and reducing sugars, which play important role in the synthesis and characteristics of

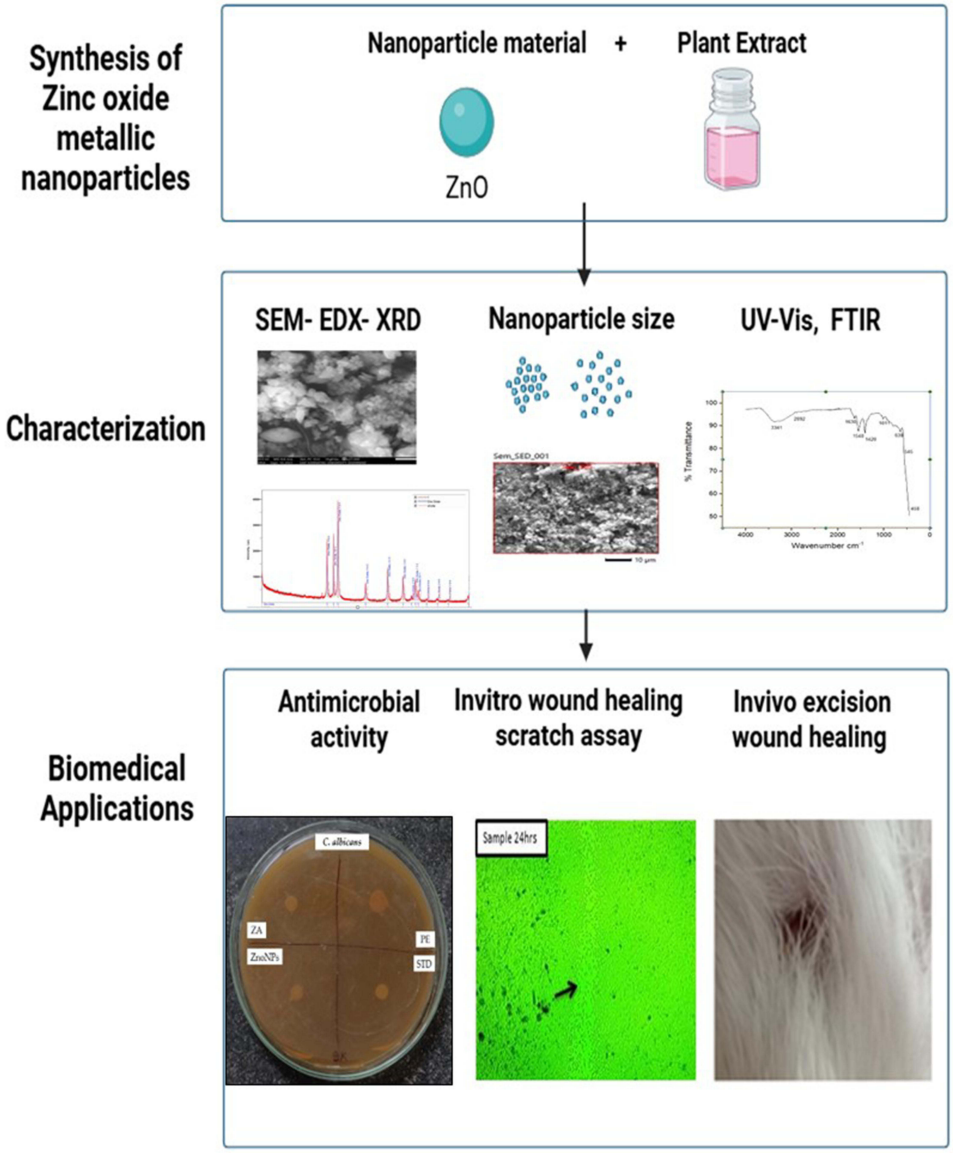

Figure 1 Synthesis, characterization and applications of ZnONPs synthesized from *S. obvallata* flowers aqueous extract.

ZnONPs.[29] By harnessing these natural compounds, this research aims to develop ZnONPs that not only exhibit potent antimicrobial and wound healing properties but also offer a safer and more sustainable alternative to existing treatments. The increasing prevalence of antimicrobial resistance, wound infections, and the need for effective wound healing agents necessitate the exploration of innovative solutions. Moreover, the findings from this study could contribute to a deeper understanding of the therapeutic applications of ZnONPs in wound care, potentially leading to improved clinical outcomes and a reduction in antibiotic resistance associated with conventional treatments. Further investigation into the mechanisms of action will provide insights that could inform future research and clinical applications.

Materials and Methods

Plant Collection and Preparation of *S. obvallata* Flower Aqueous Extract

S. obvallata flowers were collected from Dharwad, Karnataka during June-July 2023. The flowers were identified by Dr. Harsha Hegde. A voucher specimen (RMRC-1877) is submitted to ICMR-National Institute of Traditional Medicine, Belagavi, Karnataka, India. A fine razor blade was used to separate the parts of the flowers and were thoroughly washed

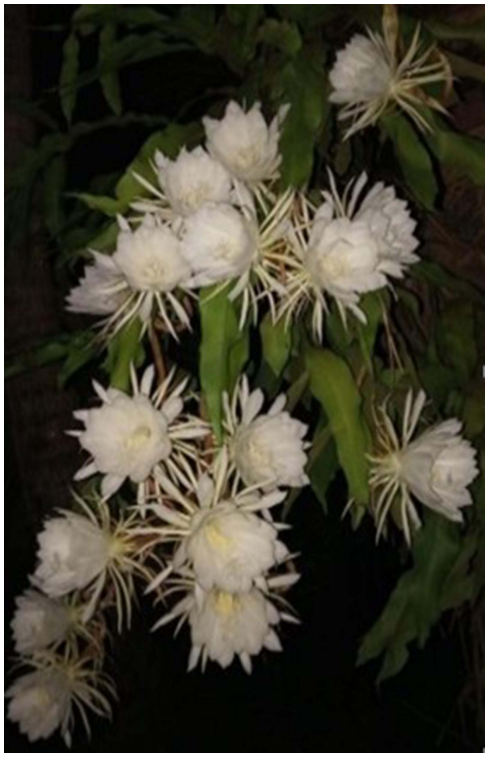

Figure 2 The flowers of *S. obvallata* (Brahma Kamala) plant.

using distilled water. The cleansed flowers were cut into small pieces. 50 g of chopped flowers were ground using pestle and mortar and then boiled in clean and sterile glass beakers containing 500 mL distilled water for 15 minutes. After boiling, the flower extracts were allowed to cool and later filtered using Whatman filter paper. The filtrate was then centrifuged at 6000 rpm for 15 minutes. The supernatant was obtained in a tube and stored in the refrigerator until further use.

Preliminary Phytochemical Screening

The standard biochemical methods were used to determine the presence of alkaloids, flavonoids, saponins, cholesterol, phenols, glycosides, anthraquinones, steroids, triterpenoids, coumarins, diterpenes, catechin, anthocyanosides, resins, and volatile oil.[29–37]

Zinc Oxide NPs Synthesis

Zinc acetate ($C_4H_6O_4Zn{\cdot}2H_2O$) was used as a substrate to synthesize ZnONPs from the flower extract. Zinc acetate (10.975 g) was added to 500 mL distilled water to obtain 0.1M zinc acetate solution. It was placed in magnetic stirrer for 1 hour for complete solubilization. 125 mL of flower extract was added drop wise to 500 mL of 0.1M zinc acetate on the magnetic stirrer and was stirred continuously. After 1 hour, the solution's pH was raised to 10 using 2M NaOH solution. The solution formed a white precipitate. The beaker was then kept in water bath at 50°C for 1 hour and later stirred continuously for 2 hours. The precipitate was allowed to settle, and it was repeatedly washed with distilled water till a pH of 7 was attained. The precipitate was then dried in the hot air oven. The dried precipitate was stored in powder form until further analysis.[23] A schematic representation of biosynthesis of ZnONPs, characterization and biomedical application is shown in Figure 3.

Characterization and Analysis of ZnONPs

The characterization of ZnONPs has grown in significance because they can be produced through various mechanical or chemical processes and have a huge potential for technological applications as well as academic research interests in a variety of fields.[38] The characterization of ZnONPs is crucial to knowing their distinctive features at various molecular

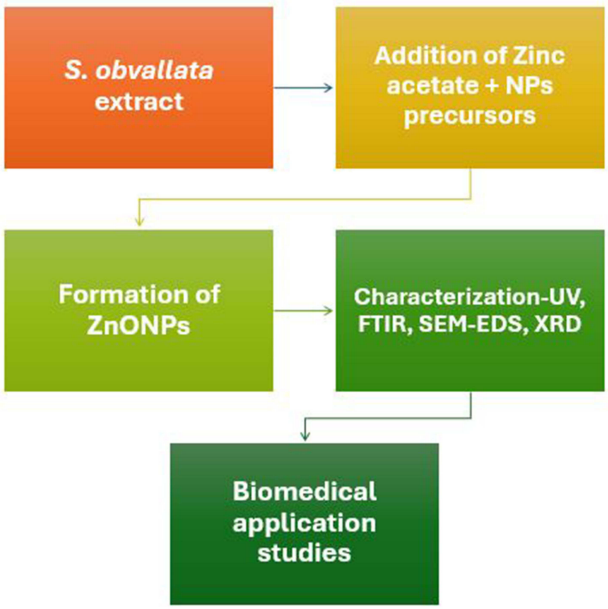

Figure 3 Schematic representation of biosynthesis of metal NPs, characterization and application studies.

levels because NPs have a huge ratio of surface area to volume, which causes their properties to change considerably with size. The crystalline phase, crystal defects, texture, shape anisotropy, crystal size, and other properties influence the chemical, electronic, mechanical, and optical characteristics of the NPs.

UV-Visible Spectroscopy

The most popular method and most straightforward way to verify the creation of NPs is UV-visible spectroscopy.[39] After dissolving 10 mg of dry precipitate in 10 mL of distilled water, the spectra of absorbance between 200 and 800 nm were measured using a Shimadzu UV-1800 spectrophotometer. To modify the baseline, distilled water was utilized as a blank. Using a graph of absorbance v/s wavelength, the wavelength with the highest absorbance was investigated.

Analysis by FTIR

To determine whether potential biomolecules were present in the sample, FTIR measurements were performed. FTIR provides a validation of functional groups qualitatively. This methodology uses reflectance and absorption spectroscopy in the IR spectral region. In this electromagnetic domain, a molecule is stimulated to reach a higher vibrational state, which is known as a vibrational transition.[40] Changes in functional groups can be used via the FTIR technique, a kind of spectroscopy, to detect variations in the general composition of biomolecules. The molecular spin and vibration impacted by an infrared wavelength are measured using FTIR. It is possible to ascertain the existence of these interactions by identifying structural changes in molecule binding.[40,41]

SEM with EDS Analysis

The ZnONPs' size, shape, and surface area were assessed using a SEM. Particle imaging is made possible by high-resolution SEM imaging, and elemental and chemical properties of the NPs can be determined by EDS. With SEM-EDS, information about the material's external morphological characteristics, composition, chemical makeup, and orientation can be acquired (manufacturing JEOL model number JSM-IT500L). Following their dehydration, the samples were examined using an electron beam, allowing ZnONP size and image data to be obtained.[42]

X-Ray Diffraction (XRD) Analysis

In order to determine crystal structure, phase composition, and crystallinity, X-ray Diffraction (XRD) experiments were carried out using a PAN analytical Xpert Pro. diffractometer with Cu-Kα radiation, employing a range of 20–80° with

a scan speed of 8° min^{-1}.[40] Scherrer's equation was used to calculate the size of the NPs. The formula is D = 0.9 / cosh, where D is the crystal size, k is the X-ray beam's wavelength, h is the Braggs angle expressed in radians, and B is the absolute width of the peak at half maximum expressed in radians.[43]

Biomedical Applications of ZnONPs

Anti-Microbial Activity

The agar disk diffusion method was employed to assess the anti-microbial susceptibility of ZnONPs and flower extract against various microorganisms.[44] *Escherichia coli, Bacillus subtilis, Pseudomonas aeruginosa, Zymomonas mobilis* and *Streptococcus aureus* were used as test organisms and ampicillin was used as standard antibiotic. The test microorganism was inoculated into nutrient agar plates using a standardized inoculum. Whatman filter papers (around 5 mm in diameter) were soaked in the test solutions (flower extract and 10 mg ZnONPs in 10 mL distilled water) for 3–4 hours prior to the inoculation. Next, the filter paper disc was put on top of the agar. The petri plates were kept in an incubator at 37°C for 24 hours. The test microorganism is seeded into the agar medium, and the test plant extract diffuses through it.[39] After incubation, if the isolated components or plant extracts under investigation are microbiologically active, a zone of inhibition will form around the filter paper disc. Antimicrobial agents that infiltrate into the agar usually hinder the germination and division of the test microorganism. The inhibitory zone's diameter provides an accurate description of how well plant extracts or compounds work against bacteria.[45]

Anti-Fungal Activity

ZnONPs and floral extract were tested for their antifungal susceptibility to the fungus *Candida albicans* using the agar disc diffusion method. *C. albicans* was inoculated into potato dextrose agar (PDA) plates using a standardized inoculum, and fluconazole was utilized as the standard antibiotic. Prior to the inoculation, Whatman filter papers with a diameter of approximately 5 mm were soaked for three to four hours in the test solutions, which consisted of floral extract and 10 mg ZnONPs in 10 mL distilled water. Next, the filter paper disc was put on top of the agar. The petri plates were kept in an incubator at 37°C for 24 hours. The agar medium that has been seeded with the test fungus diffuses the test plant extract across it.[44] After incubation, if the isolated components or plant extracts under investigation are microbiologically active, a zone of inhibition will form around the filter paper disc. An antifungal drug that diffuses into the agar usually inhibits the fungi's germination and proliferation. The diameter of the inhibitory zone provides an accurate description of how well plant extracts or compounds work against bacteria.[8,45–48]

In vitro Wound Healing Scratch Assay Test

The current work examined the spreading and migratory characteristics of the L929 cell line-induced samples using a known concentration of metallic NPs synthesized from *S. obvallata*.[49] At first, the cells were cultured on 12-well animal cell culture plates supplemented with 10% FBS and 2% penstrip antibiotic in DMEM media. Once the growth reached a complete density of about 50,000 cells, or the development of a monolayer confluent of cells, a scratch was produced with a sterile 100 µL plastic pipette tip. PBS solution helped wash away unwanted cell debris. Additionally, the cells were treated with various testing polymer samples that had been quantified. Untreated cells were used as the negative control, and standard ascorbic acid was used as the positive control. After that, the cells were cultured for 24 hours at 37 °C with 5% CO_2. The scratched cell layers were imaged and utilised to examine relative cell migration and wound closure. The cells were cultured at various intervals starting at 0 hours, 12 hours, and 24 hours. Using measurement calibration at 4X resolution and MagVision software, the gap distance was quantitatively assessed. The following formula was used to determine the rate of migration and wound closure:

Wound closure (%) = $A_{0h} - A_{Th}/ A_{Th} \times 100$

Rm (Rate of migration) = $W_i - W_f/T$

Wherein A_{0h} = Area of the wound was measured immediately after scratching, A_{Th} = Area of the wound measured after the scratch is performed h hours, Rm = Rate of migration (µm/h), W_i = Initial wound width (µm); W_f = Final wound width (µm) and T = Duration of migration (hour).

In vivo Wound Healing Activity

Experimental Animals and Grouping

Wistar rats weighing between 180 to 200 g of both sexes, were employed in this study. The animals were kept at a temperature of about 22°F under controlled settings. They were housed in husk-lined polypropylene cages and the husk was replaced every twenty-four hours. Food and water were freely available to the rats. A standard pellet diet was given to the rodents. The Ethical approval was obtained from the Najran University Scientific Research Ethical Committee. The animals were randomly divided into 3 groups, with six animals (n = 6) in each group. Group I was designated as control (received ointment base only); Group II was treatment group (received ZnONPs ointment 5% W/W); and Group III was standard (received povidone-iodine ointment 5% W/W).

Formulation of ZnONPs Loaded Ointment

An ointment was formulated following a formula in the British Pharmacopoeia, which included white soft paraffin, cetostearyl alcohol, hard paraffin, and wool fat.

Procedure. The ingredients were added in a specific order based on their melting points: cetostearyl alcohol (5 g), white soft paraffin (85 g), and wool fat (5 g) to create the 100 g simple ointment base. All the components were melted in a water bath with continuous stirring until they formed a uniform mixture. The mixture was removed from the heat source and stirred until it reached room temperature. The ZnONPs containing ointment was prepared by combining five grams of *Saussurea obvallata* ZnONPs with a portion of the simple ointment base to create a 5% (w/w) ointment. The remaining ointment base was slowly added and mixed well. The ointment was carefully stored in a clean and dry container, kept away from sources of heat. The ointment was applied topically to the wounds for 24 consecutive days throughout the study.

Excision Model Wound Healing Activity

An incision was made on anesthetized albino rats following the excision wound model protocol. Anesthetics were administered to the rats to induce anesthesia before causing the wound injury. Ketamine was given at a dose of 80 mg/kg and diazepam at 5 mg/kg i. p. An excision wound in the shape of a circle, measuring around 500 mm^2 and 2 mm deep, was created on the shaved area of the upper back. Thereafter, based on the grouping and dosing section, ointments with ZnONPs (test group) and without medication (control group) were applied topically on a daily basis. The day the injury initiated was considered as day 0. During specific time points after the wound was created, we observed the wound area's closure and period of epithelialization. By utilizing the equation, the percentage of the extracts' wound contraction effect was determined based on the initial size of the wound. The duration of epithelization was established by tracking the number of days until the wound no longer showed any raw tissue after the dead tissue had shed off.

$$\%\ \text{of wound closure} = \frac{\text{wound area on day 0} - \text{wound area on day } n}{\text{wound area on day 0}} \text{X}100$$

Estimation of Hydroxyproline Content

On the twenty-first day of the experiment, the hydroxyproline content in the excised wound tissues was evaluated. The tissue samples were dried in a hot air oven set at 60°C. Following this, they were subjected to hydrolysis for four hours at a temperature of 130°C with 6 N hydrochloric acid. After neutralizing the hydrolysates to a pH of 7.0, they were oxidized with Chloramine-T for 20 minutes. The experiment was stopped after 5 minutes by adding 0.4 M perchloric acid, and then Ehrlich's reagent was used to develop color at 60 °C. The samples underwent analysis with an ultraviolet spectrophotometer at a wavelength of 557 nm after being thoroughly agitated. The level of hydroxyproline in the tissue samples was determined using a standard curve of pure L-hydroxyproline.[50]

Histopathology

On the 21st day of the wound healing experiment, the animals were anesthetized with Ketamine hydrochloride (50 mg/kg, i.p). before being euthanized. Subsequently the samples of the wound tissue and the adjacent healthy tissue were

collected. After being fixed in 10% formalin, the collected samples were subjected to a standard histopathological tissue examination. The wound tissue specimen was stained using Hematoxylin-eosin. We utilized a light microscope to analyze the prepared tissue slide. The sample of wound tissue was sliced into sections, treated with a dye that targets collagen fibers known as Van-Gieson stain, and analyzed under a microscope to assess its collagen levels.

Results and Discussion

Preliminary Phytochemical Screening

The preliminary phytochemical screening revealed the presence of secondary metabolites like alkaloids, flavonoids, saponins, steroids, to name a few. The results are depicted in Table 1.

Characterization of ZnONPs

In contemporary nanotechnology, the synthesis and utilization of nanomaterials are highlighted. A variety of secondary metabolites, such as phenolic compounds, terpenoids, essential oils, flavonoids, and other natural products, are found in plants, including herbs, lower plants, higher plants, weeds, roots, and more.[51] Green synthesis of NPs is preferred to physical and chemical procedures since it is simple, environmentally benign, affordable, and free of any toxic components or poisonous organic solvents. Physical-chemical methods for producing NPs are expensive, dangerous to the environment, and require high temperatures and pressures. Because dangerous chemicals can occasionally stay deposited on the surface of NP, these NPs not suitable to be employed in biomedical settings. *S. obvallata* was used in the current study to produce ZnONPs. This plant was chosen for its phytochemical content. These biomolecules may be involved in ZnONPs capping, stabilization, and reduction. ZnONPs have previously been made using a variety of medicinal plants. In the current experiment, *S. obvallata* flower extract was used to create ZnONPs. The zinc acetate and *S. obvallata* flower extract solution mixture's colour changed from pale brown to yellowish during the bio-synthesis of ZnONPs. The transformation of

Table 1 Phytochemical Screening of *S. obvallata* Flower Aqueous Extract

S. No	Phytochemical Tests	Results
1.	Alkaloids	+
2.	Flavonoids	+
3.	Saponins	+
4.	Steroids	+
5.	Triterpenoids	–
6.	Tannins	–
7.	Phenols	–
8.	Glycosides	–
9.	Anthraquinones	–
10.	Coumarins	+
11.	Diterpenes	+
12.	Catechins	+
13.	Anthocyanosides	–
14.	Resins	+
15.	Volatile oil	+

metallic zinc (Zn+) ions into zinc (ZnO) NPs was indicated by this colour shift. The resultant greyish substance, which was later employed for physical characterizations and thought to be ZnONPs, was obtained.

UV-Vis Spectrophotometer

An optical UV-4000 UV-Vis spectrophotometer (Germany) was used to measure the reaction solution's UV-absorption at wavelengths between 200 and 800 nm to track the reduction of zinc ions. The creation of ZnONPs is indicated by the absorbance band at 370 nm (max) in Figure 4. Since the dimension, structure, concentration, aggregated state, and refractive index (RI) at the NP surface may all affect an object's optical characteristics, UV/Vis/IR spectroscopy is a useful tool for identifying, characterizing, and researching these materials.[46] In order to monitor the shift of zinc ions into NP form, measurements of the solutions' UV-visible spectra were made.

FTIR Analysis

The bioactive components in aqueous *S. obvallata* flower extract were analysed using FT-IR to determine their contribution to ZnONPs synthesis. In the field of natural products, the IR spectroscopic approach is also utilized to identify specific biomolecules. Different infrared bands are visible, showing that biomolecules with numerous functional groups have settled on the surface of ZnONPs. These biomolecules acted as stabilizers and reducers, confirming the

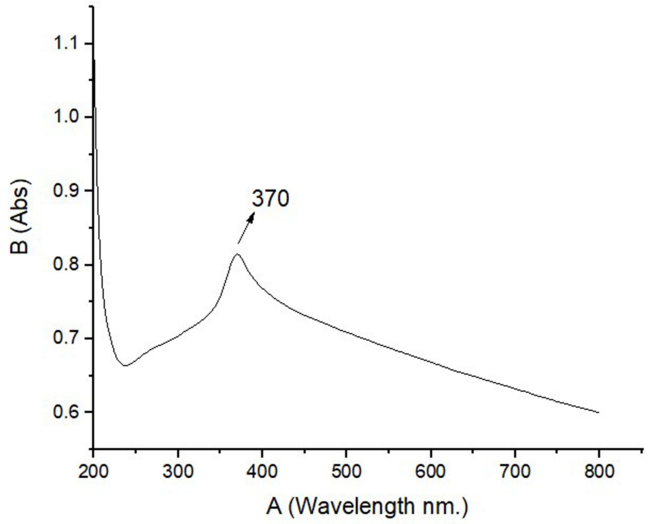

Figure 4 UV-Vis Spectra of ZnONPs synthesized from *S. obvallata* flower extract.

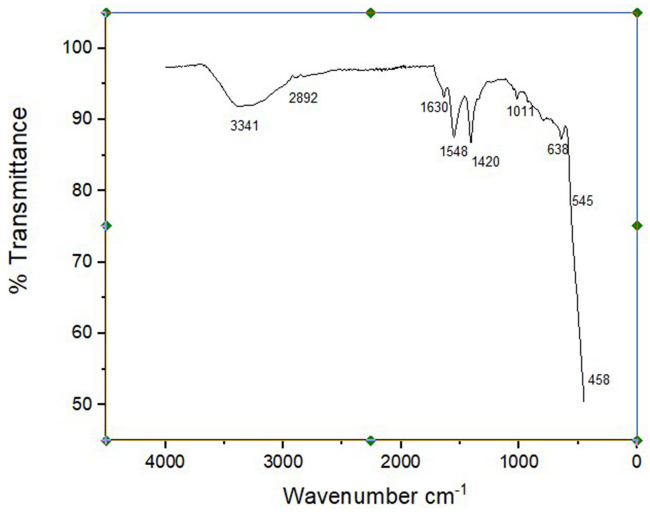

Figure 5 FTIR Spectra of *S. obvallata* flower extract showing characteristic peaks.

synthesis of ZnONPs (Figure 5). Peaks at 458 cm^{-1} and 638 cm^{-1}, for example, show Zn-O stretching vibrations; 1420 cm^{-1} corresponds to "C=C" stretching vibrations; 2892 cm^{-1} corresponds to C-C and -C-H stretching vibrations; and 3341 cm-^{1} refers to alcohols and phenols of OH stretching. These peaks indicate the presence of numerous biomolecules previously found.[41] Previous research has suggested that the IR bands between 470 and 800 cm^{-1} are generated by Zn-O stretching vibrations.[37,38] This makes the case for the use of plant-based extracts as environmentally benign agents in the synthesis of nanoparticles, as they offer a sustainable source and functional bio-compounds necessary for the stable and regulated synthesis of zinc oxide nanoparticles. This new perspective enriches our understanding of how sustainable alternatives to chemical procedures can be provided by natural product-based approaches.

Scanning Electron Microscopy with Energy Dispersive Spectroscopy (SEM EDS)

The EDX spectrum of the synthesized ZnONPs is shown in Figure 6, and the robust signal supported the production of pure metallic ZnONPs. The carbon and oxygen signals, that could have originated from bioactive substances, serve as stabilizing agents at the surface of ZnONPs. Additionally, just the peaks for the elements "Zn" and "O" were seen, supporting the phase purity of EA-ZnONPs.

Scanning electron microscopy (SEM) was used to analyze the morphology and form of the green synthesized ZnONPs. Most of the morphology of EA-ZnONPs is spherical/agglomerated, and typical SEM images are shown in Figure 7. SEM with EDS is one of the most popular methods for describing NPs. These procedures are necessary since optical microscopes are unable to observe them due to their small size (1–100nm). EDS provides elemental and chemical information about the NPs, and high-resolution imaging in SEM enables imaging of the particles.[42] The sample material releases x-rays that are unique to the elements it contains after being exposed to electron radiation. The energy emissions are converted into spectral peaks of different strengths to create the spectrum profile. As seen in Figure 6, the ZnO powder's EDX characterization indicates that it is a high-purity compound with high Zn and oxygen concentrations.[43]

X-Ray Diffraction

XRD tests were carried out to determine the phase purity and crystallinity of ZnONPs. Figure 8 shows XRD patterns of ZnONPs with diffraction bands corresponding to fcc symmetry in the ZnONPs crystalline lattice at 32.37 (100), 34.14 (002), 36.72 (101), 46.79 (102), 57.75 (110), 65.61 (103), 68.14 (112), and 69.94 (201). Wide peaks in the XRD pattern highlighted the particle's small size and determined how the experimental conditions affected crystal nuclei nucleation and development. The crystalline structure of the ZnONPs synthesized corresponds to the gold standard defined by JCPDS Data Card No: 36–1451). The size of XRD determined by applying the Scherrer equation agreed with the ZnONPs size values. The average size of ZnONPs is 28.33 nm (Table 2). The XRD method is flexible to accurately analyze and gather data on the chemical arrangement, structural grain size, and crystallographic structure of NPs. The Powder XRD analysis provides valuable information that complements a range of microscopic and spectroscopic techniques. Some examples of the information provided in these publications are phase identification, sample purity, crystallite size, and, in certain cases, morphology. The XRD method operates on the basis of the scatter of X-rays induced by the revolution of atoms' electrons in their nuclei when the beams strike the NPs. The disseminated X-rays reflect in different ways, which leads to patterns of interference. Diffraction only occurs when dispersed X-rays interact constructively, regardless of whether these patterns are destructive or constructive.[43]

Biomedical Application Studies of ZnONPs Synthesized from S. obvallata Flower Extract

Anti-Microbial Activity

Bacterial infection, which results from harmful bacteria invading the host, is a common cause of mortality and morbidity and an urgent health problem in the world.[52] The antibacterial activity of ZnONPs and the aqueous flower extract in combination with antibiotic ampicillin was tested against gram positive organisms like *B. subtilis and S. aureus* and gram-negative organisms like *E. coli, P. aeruginosa and Z. mobilis* (Figures 9 and 10). Agar disc diffusion assay method was employed. Ampicillin was used as standard antibacterial agent. The results of the antimicrobial assay are depicted in Table 3 and statistical analysis is shown in Figure 10.

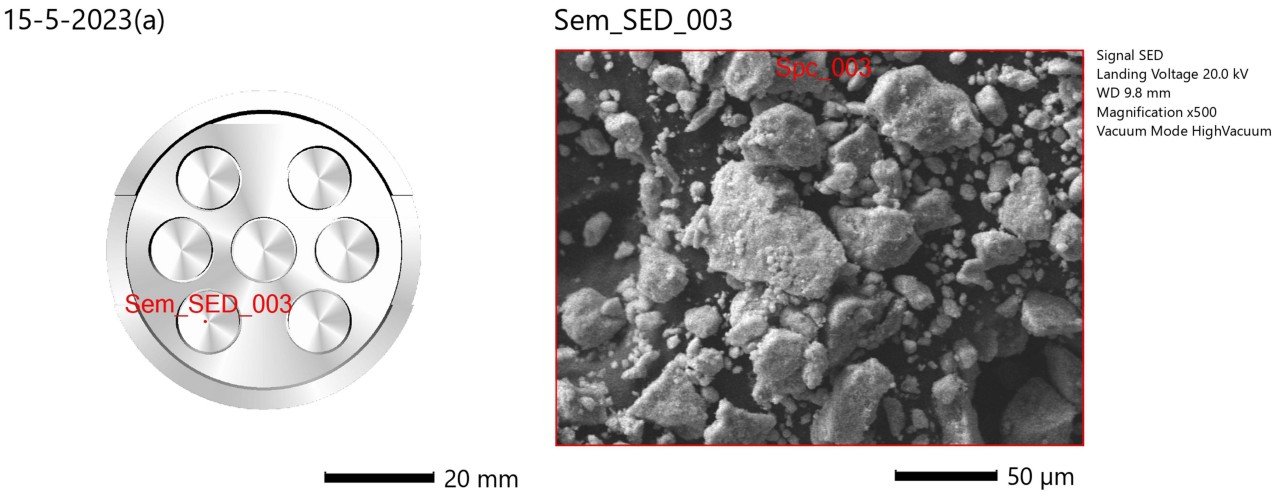

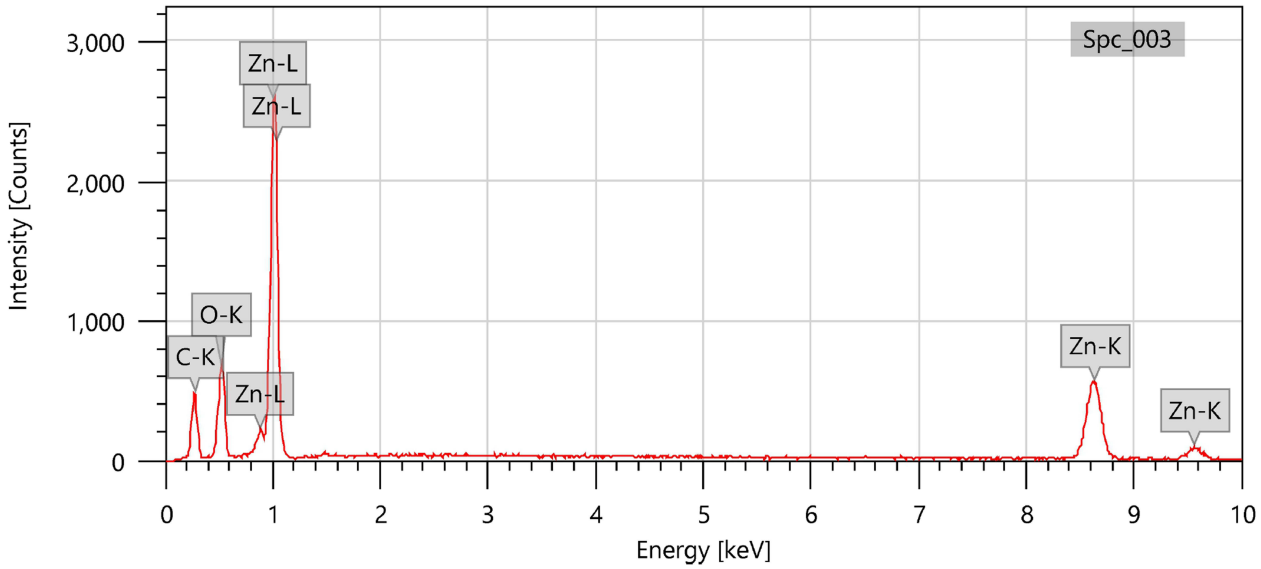

Items	Value
measurement conditions	
Acceleration voltage	20.00 kV
Probe current	0.00 nA
Magnification	x 500
Process time	T3
Measurement detector	First
Live time	30.00 seconds
Real time	30.79 seconds
Dead time	3.00
Count rate	2226.00 CPS

Display name	Standard data	Quantification method	Result Type
Spc_003	Standardless	ZAF	Metal

Element	Line	Mass%	Atom%
C	K	27.55±0.22	52.10±0.42
O	K	21.19±0.26	30.08±0.37
Zn	K	51.26±0.58	17.81±0.20
Total		100.00	100.00
Spc_003			Fitting ratio 0.0291

Figure 6 SEM-EDS Spectra of ZnONPs synthesized from *S. obvallata* flower extract.

Anti-Fungal Activity

The antifungal activity of ZnONPs and the aqueous flower extract in combination with antibiotic fluconazole was tested against *C. albicans*. Agar disc diffusion assay method was employed. Fluconazole was used as standard antifungal agent. The zone of inhibition observed was 16 mm for ZnONPs and 12 mm for Zinc acetate (Table 4, Figures 10 and 11).

At 0.1M concentration, zinc acetate inhibited *C. albicans* with a zone of 12 ± 0.50 mm. This implies that zinc acetate has antifungal effects and can limit fungus development to a moderate amount. ZnONPs had a bigger inhibitory zone of 16 ± 0.2 mm compared to zinc acetate. This shows that ZnONPs have a higher antifungal effect on *C. albicans* than zinc

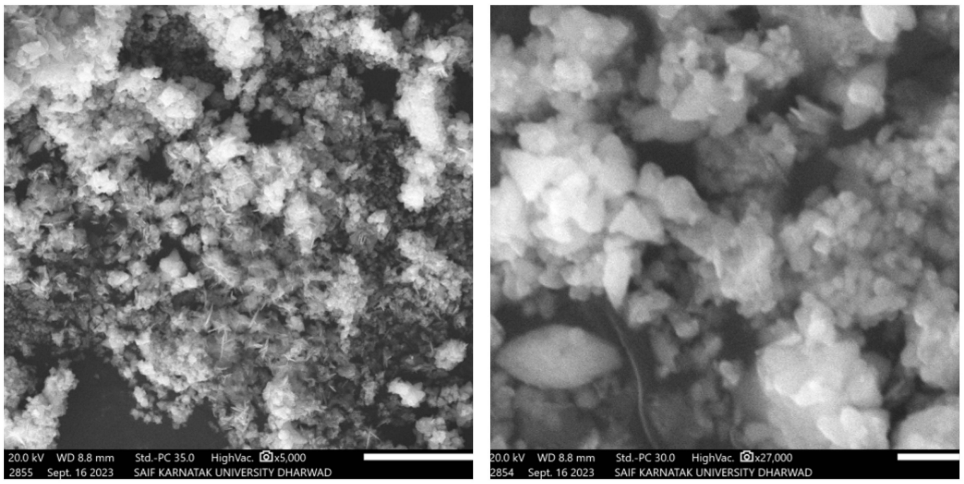

Figure 7 SEM image of ZnONPs synthesized from *S. obvallata* flower extract.

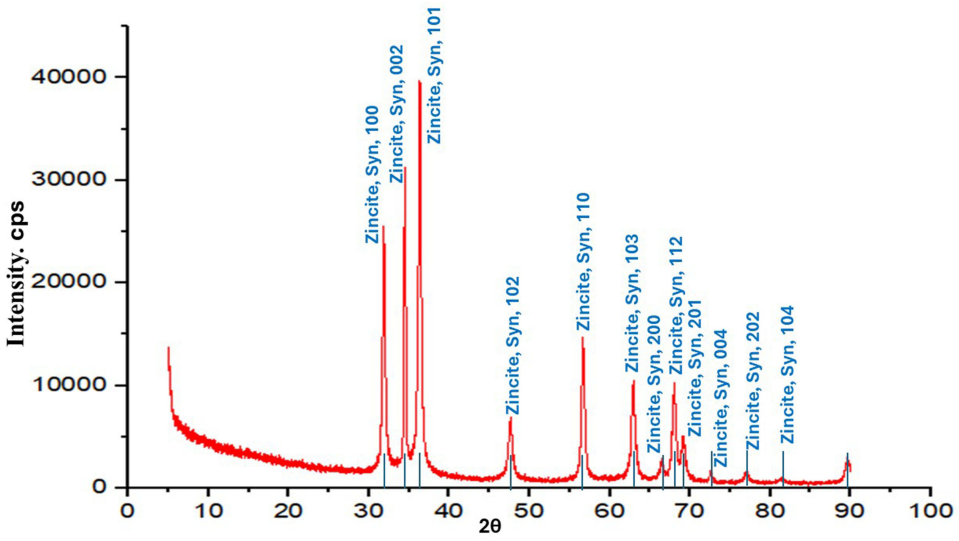

Figure 8 XRD Spectra of ZnONPs synthesized from *S. obvallata* flower extract.

acetate. The plant extract showed a zone of inhibition of 13 mm, and the NPs had an increased inhibitory action (16 mm), indicating their potential as an effective antifungal agent. The study used the antibiotic fluconazole as a reference. Fluconazole exhibited a significant inhibitory zone of 35 ± 0.3 mm against *C. albicans*, demonstrating strong antifungal properties. This finding verifies fluconazole's effectiveness as a typical treatment for *C. albicans* infections. The findings indicate that both zinc acetate and ZnONPs have antifungal efficacy against *C. albicans*, with ZnONPs exerting a slightly higher inhibitory impact.

By preventing or reducing microbial colonization in the wound, ZnONPs treated wounds provide a cleaner and more sterile environment for the healing process to occur. This can minimize the inflammatory response and prevent the formation of biofilms, which are notorious for impeding wound healing. Additionally, the antimicrobial activity of ZnONPs can help prevent secondary infections and complications that can further delay the healing process. The potent antimicrobial activity exhibited by ZnONPs in the current study can be linked to their enhanced wound healing

Table 2 XRD Data and Crystalline Size of ZnONPs Synthesized from *S. obvallata* Flower Extract

Sl. No.	2θ (In Degrees)	2θ (In Radians)	FWHM (In Degrees)	FWHM (In Radians)	Crystalline Size (nm)
1	22.55472	0.393654	0.1183	0.002065	68.47589
2	29.71775	0.518673	0.1087	0.001897	75.613
3	31.68862	0.553071	0.3282	0.005728	25.16159
4	32.19091	0.561837	0.4372	0.007631	18.91217
5	34.39163	0.600247	0.2243	0.003915	37.07541
6	36.22133	0.632181	0.3367	0.005877	24.82442
7	47.49367	0.828921	0.4313	0.007528	20.12316
8	56.55725	0.98711	0.3941	0.006878	22.88986
9	62.75297	1.095246	0.4809	0.008393	19.34916
10	66.35176	1.158057	0.4171	0.00728	22.7558
11	67.88998	1.184904	0.4777	0.008337	20.04678
12	69.03049	1.204809	0.5101	0.008903	18.90103
13	72.55155	1.266263	0.3082	0.005379	31.97357
14	76.9763	1.34349	0.6069	0.010592	16.7233
15	81.30833	1.419098	0.7641	0.013336	13.7044
16	89.55468	1.563024	0.6622	0.011558	16.9005

properties. The antimicrobial activity of ZnONPs helps create a favorable environment for wound healing by preventing or controlling microbial infections, which are known to delay the healing process.[53]

In vitro Wound Healing Assay

One of the methods used to assess the effects of the NPs in wound healing is the scratch assay. The scratch assay is a simple and popular in vitro method for examining cell migration and wound closure. In the present study the known concentration (15µg) metallic ZnONPs synthesized from *S. obvallata* were used on L929 cell line along with standard ascorbic acid (5µg) as positive group. The results revealed that cell migration was observed highest with standard drug ascorbic acid followed by ZnONPs than untreated group of cells (Table 5). The percentage of wound closure studies showed that as the duration increases the percentage of wound closure was increased. After 24 hrs of incubation in case of standard ascorbic acid the percentage of wound closure was observed to be 93.45%, for test sample metallic NPs it was found to be 84.70% and for untreated group it has seen around 8.12% (Table 6 and Figure 12).

Soft tissue abnormalities resulting from trauma, burns, chronic disease complications, or procedures that cannot be primarily closed can cause significant morbidity and mortality.[54] A wound is a disruption in the continuity of the body's tissues, often resulting from injury, trauma, surgery, or other causes. Wounds can vary greatly in their severity, causes, and the way they are managed. There are several different ways to classify wounds based on various factors, including their cause, depth, contamination, and healing process.[55] Managing wounds involves a combination of wound care, infection prevention, and sometimes surgical intervention. Treatment can include cleaning the wound, removing debris, applying dressings or wound covers, administering antibiotics if necessary, and ensuring proper wound healing conditions.

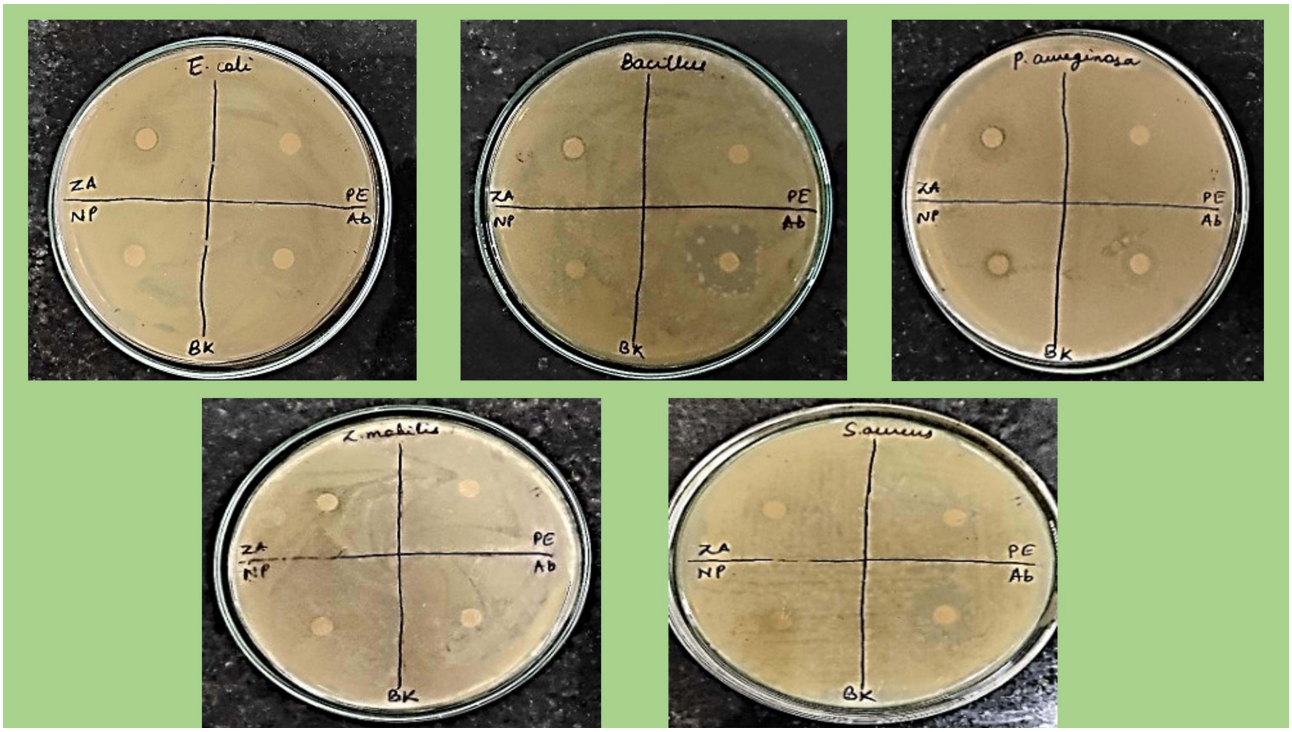

Figure 9 Antibacterial activity of ZnONPs against pathogenic bacteria.

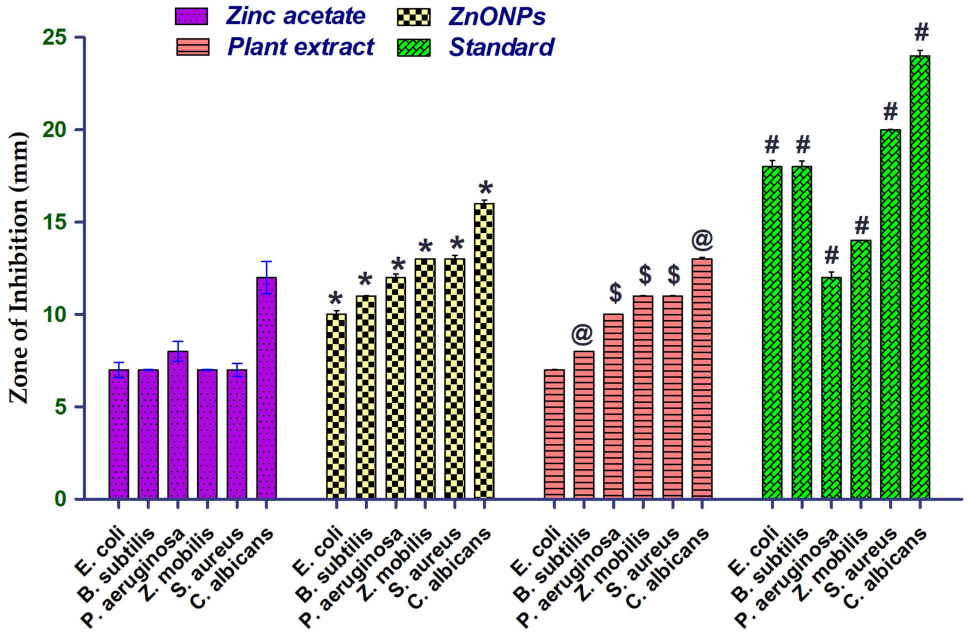

Figure 10 Antibacterial and antifungal activity of *S. obvallata* synthesized ZnONPs. Mean ± SEM for 3 readings. Statistical significance at * $p < 0.001$ compared to Zinc acetate and Plant extract; $^{@}p < 0.01$, $^{\$}p < 0.001$ compared to Zinc acetate; $^{\#}p < 0.001$ compared to Zinc acetate and Plant extract. Two-way ANOVA followed by Bonferroni post tests for multiple comparisons.

Table 3 The Antibacterial Activity of ZnONPs and the Aqueous Flower Extract in Comparison with Standard Antibiotic

	Zinc Acetate (0.1M)	ZnONPs	*S. obvallata* Extract	Standard (Ampicillin)
Escherichia coli (Gram Negative)	7 ± 0.23 mm	10 ± 0.22 mm	7 ± 0.01 mm	18 ± 0.33 mm
Bacillus subtilis (Gram Positive)	7 ± 0.01 mm	11 ± 0.01 mm	8 ± 0.02 mm	18 ± 0.31 mm
Pseudomonas aeruginosa (Gram Negative)	8 ± 0.31 mm	12 ± 0.2 mm	10.0 ± 0.02 mm	12 ± 0.3 mm
Zymomonas mobilis (Gram Negative)	7 ± 0.02 mm	13 ± 0.01 mm	11.0 ± 0.03 mm	14 ± 0.01 mm
Streptococcus aureus (Gram Positive)	7 ± 0.2 mm	13 ± 0.2 mm	11 ± 0.02 mm	20 ± 0.31 mm

Table 4 The Antifungal Activity of ZnONPs Against C. Albicans

	Zinc Acetate (ZA) (0.1M)	ZnONPs	Plant Extract (PE)	Standard (STD) (Fluconazole)
Candida albicans	12 ± 0.50 mm	16 ± 0.2 mm	13 ± 0.1	24 ± 0.3 mm

Wound healing is a complex biological process that the body initiates to repair damaged tissue. While the body's natural mechanisms are often effective in healing wounds, there are situations where wound healing can fail or be impaired. Treatment failures in wound healing can occur due to various factors, and they can be broadly categorized into local and systemic factors.[56] Addressing wound healing treatment failures requires a comprehensive approach that targets both the local wound environment and systemic factors. This might involve proper wound care, infection management, addressing underlying health conditions. Metallic NPs have gained substantial focus in the area of wound healing because of their distinctive characteristics and potential applications. In the in vitro wound healing assays, ZnONPs exhibited significant activity in promoting cellular migration and proliferation, which are crucial steps in the wound healing cascade. The NPs facilitated the closure of the wound by enhancing the migration of cells into the wound area and promoting cell division and proliferation, leading to accelerated healing.

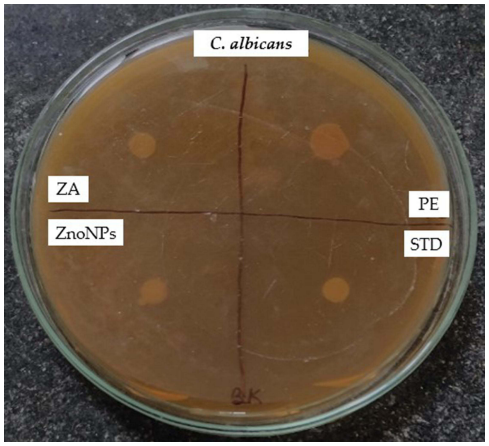

Figure 11 Antifungal activity against *C. albicans* depicting the zone of inhibition.

Table 5 Cell Migration of Different Test Samples at Different Duration

S. No	Test Sample	Duration (hrs)	Cell Migration (mm)
1	**Untreated**	6	3.56
		12	2.31
		24	1.87
2	**Ascorbic acid**	6	10.54
		12	7.32
		24	3.44
3	***S. obvallata* ZnONPs**	6	8.88
		12	5.56
		24	2.43

Table 6 Percentage of Wound Closure of Different Test Samples

Sl. No	Test Sample	Percentage (%) of Wound Closure
1	Untreated	8.12
2	Standard drug (Ascorbic acid)	93.45
3	*S. obvallata* ZnONPs	84.70

Effect of S. obvallata ZnONPs on in vivo Wound Healing

Percentage wound contraction for ZnONPs and Povidone-Iodine are depicted in Table 7. A significant ($p < 0.01$) wound contraction was observed in animals treated with ZnONPs and Povidone-Iodine on day 8 as compared to untreated animals (Excision control). Animals treated with ZnONPs and Povidone-Iodine showed nearly complete healing of the wound on day-21. Group I (Excision control) animals had an epithelization duration of 17.9 days, while ZnONPs and Povidone-Iodine treated groups animals had epithelization periods of 10.2 and 7.6 days, respectively. Complete epithelization occurred in ZnONPs and Povidone-Iodine treated groups significantly faster ($p < 0.01$) than in the control group who received no treatment. ZnONPs ointment's wound healing effect was similar to the Povidone-Iodine ointment (Figures 13 and 14). The in vivo wound healing assays further supported the beneficial effects of ZnONPs on wound healing. When applied topically, ZnONPs demonstrated a remarkable ability to improve wound closure and promote wound healing. Recent studies have shown that the enhanced wound healing by the NPs could be attributed to angiogenesis, enhanced collagen synthesis, and accelerated re-epithelialization, resulting in faster and more efficient wound healing. Experimental models have confirmed its effectiveness in promoting wound contraction, collagen deposition, and angiogenesis.[55] In a study reported by Han et al, 2012, it was found that topical application of NO-releasing nanoparticles promoted angiogenesis in mouse excisional skin wound model.[56]

Hydroxyproline Content

Figure 15 illustrates the impact of ZnONPs on Hydroxyproline content in the healed tissue. The hydroxyproline level in the excision control animals was measured at 26.39 ± 1.5. In animals treated with ZnONPs, the hydroxyproline content was found to be significantly higher (35.07 ± 1.7) compared to animals in the excision control group, with significance at $p < 0.05$. In addition, rats that received Povidone-Iodine exhibited a substantial increase in hydroxyproline content (80.86 ± 2.1) compared to the excision control animals, with statistical significance ($p < 0.001$) (Table 8).

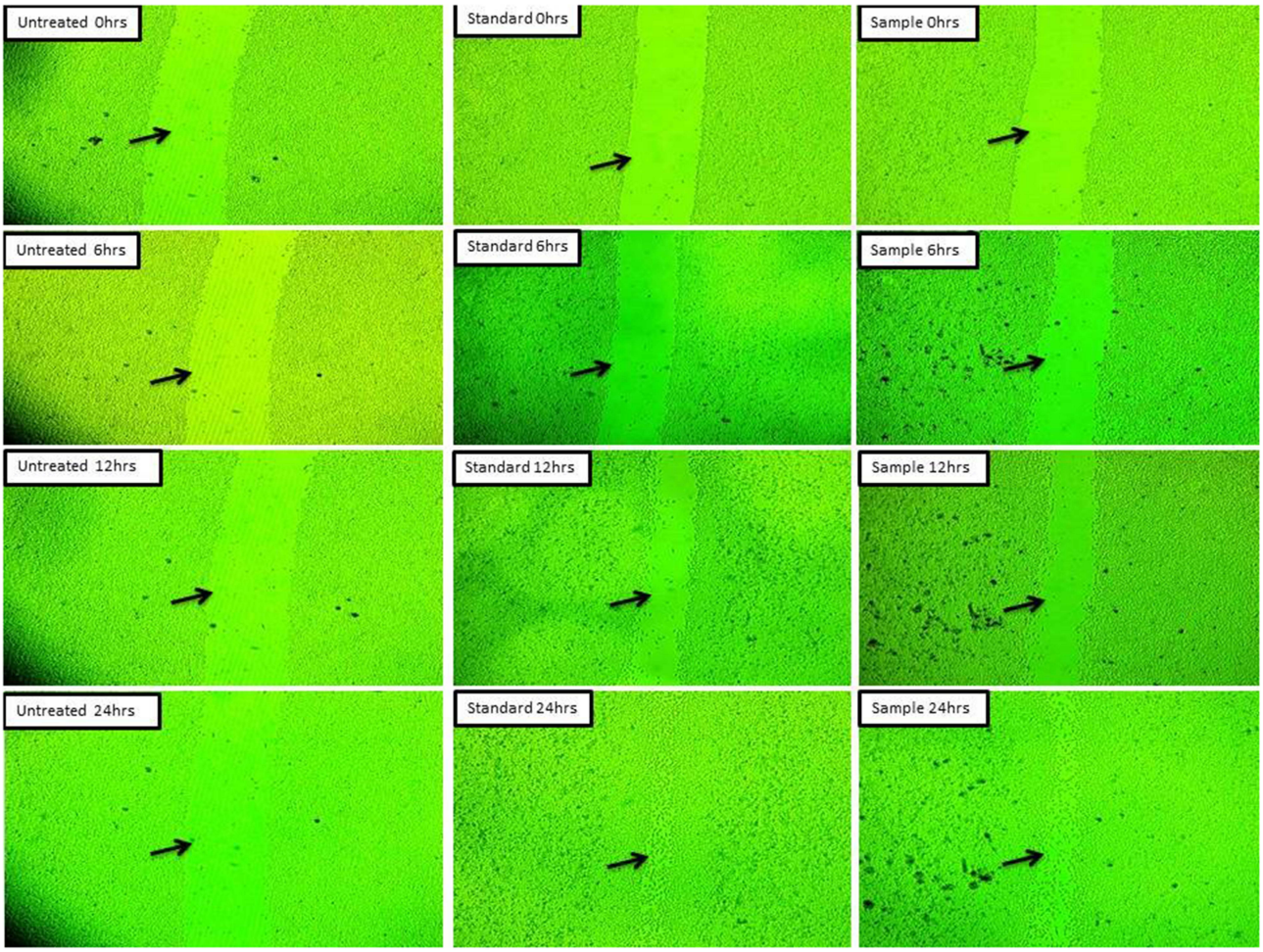

Figure 12 Microscopic study of wound closure treated by *S. obvallata* ZnONPs. The black arrows indicate the gap between the migrating cells depicting the percentage of wound closure.

Previous studies have showed that a greater content of hydroxyproline indicates faster wound healing.[57–59] The samples in the current study had higher hydroxyproline contents, which is suggestive of higher collagen synthesis and cellular proliferation, according to the biochemical analysis. Collagen provides strength and stability to the tissue matrix and is essential for homeostasis and epithelialization during the restorative process. Thus, enhanced hydroxyproline production reinforces the healing pattern and the restored tissue.[58,59]

Diabetes continues to be a serious worldwide health issue. The healthcare system is burdened by diabetic wounds, which are the primary cause of amputation in diabetic patients. The *S. obvallata* ZnONPs can be utilized to create suitable wound dressings that regulate drug release to support the growth of connective tissue and cell proliferation.[60–62]

Table 7 Hydroxyproline Content (µg/100mg of Tissue) of Treatment Groups

Sl. No	Treatment Groups	Hydroxyproline (µg/100mg of Tissue)
1	Excision (Control)	26.39 ± 1.5
2	*S. obvallata* ZnONPs	35.07 ± 1.7*
3	STD (Povidone-Iodine)	80.86 ± 2.17***

Notes: Values are expressed as Mean±SEM for 6 animals per group. *p < 0.05; ***p < 0.001 compared with control group.

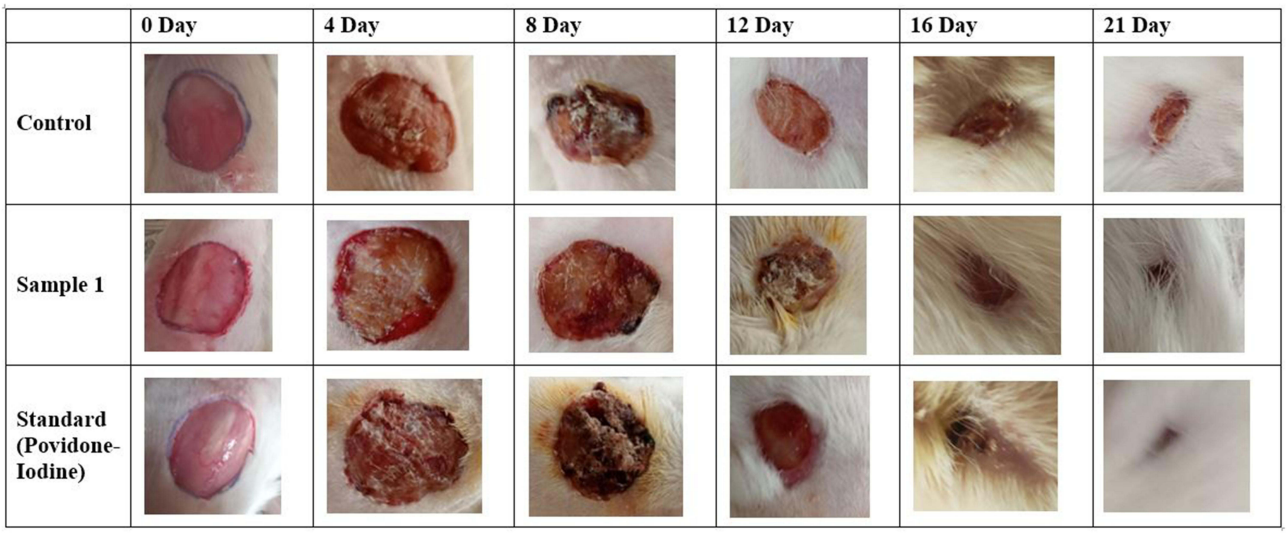

Figure 13 Images showing the impact of *S. obvallata* ZnONPs on excision wound model at different time points of the study duration.

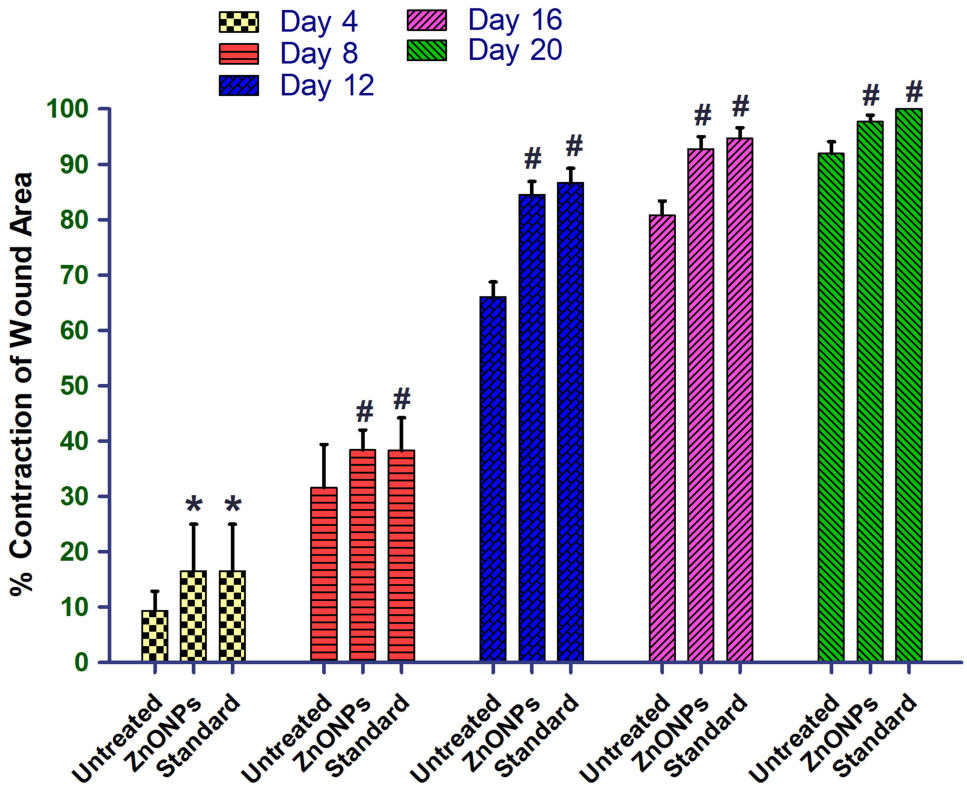

Figure 14 The percentage wound closure in the incision wound model. Values are presented as Mean ± SEM for six animals per group. *p < 0.05; #p < 0.001 versus untreated control.

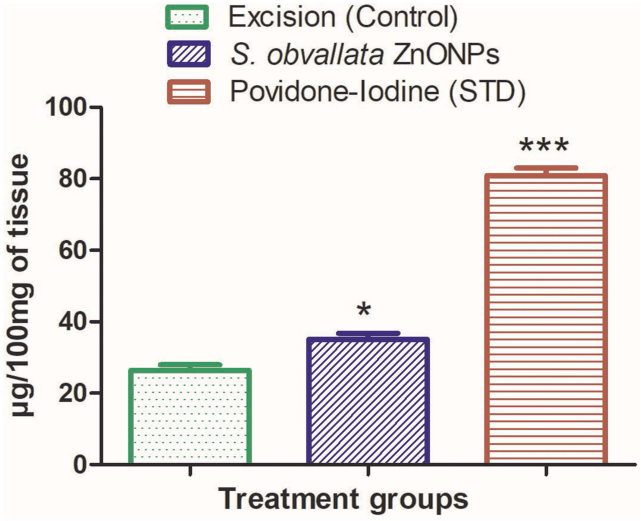

Figure 15 Effect of ZnONPs on Hydroxyproline Content (µg/100mg of tissue). Values are expressed as Mean±SEM for 6 animals per group. *p < 0.05; ***p < 0.001 compared with control group.

Histopathology Study

The rats treated with ZnONPs and the standard (povidone-iodine ointment) had extensive and well-organized collagen fibers (Figure 16). Significant injury was seen in the untreated group, such as substantial fibrosis, cellular infiltration, inflammation, and epithelial deterioration. The ZnONPs treated animals developed a thick epidermal layer, dermal granulation tissue, papillary dermis, sebaceous glands, dermal collagen, and hair follicles, whereas untreated control animals did not. Animals treated with ZnONPs showed no evidence of inflammation in the regenerated tissue, similar to those treated with the standard drug. For regenerated skin tissue, the deeper penetrability of ZnONPs ointment formulation promotes the formation of complex and well-organized cell structures. Granulation tissue is a foundation for new tissue growth and helps facilitate wound closure. Similarly, one of the most crucial elements of wound healing is collagen. It promotes epithelization from the wound edge and permits cell migration for skin restoration, which quickens the healing process. The ZnONPs treated animals exhibited higher dermal granulation tissue and collagen.

The use of flower extract in the synthesis of zinc oxide nanoparticles (ZnO NPs) confers unique properties that significantly enhance tissue regeneration and wound healing. The natural compounds present in the flower extract can improve the biocompatibility of ZnO NPs, making them safer for biological applications. Additionally, the phytochemicals in the extract provide antioxidant properties that help mitigate oxidative stress during the healing process, which is crucial for effective wound recovery. The bioactive compounds can also enhance the interaction of ZnONPs with cells, promoting better adhesion, proliferation, and differentiation of fibroblasts and other regenerative cells. Furthermore, the natural matrix from the flower extract may facilitate a controlled release of zinc ions, ensuring sustained bioactivity necessary for wound healing. Lastly, the extract is likely to contain anti-inflammatory agents that can reduce inflammation at the wound site, thereby creating a more favorable environment for wound healing.

As the world increasingly prioritizes sustainability, the movement toward achieving a negative carbon footprint has become a central focus in various sectors, including healthcare and nanotechnology.[63] By employing sustainable practices, this approach not only minimizes environmental impact but also aligns with global efforts to reduce carbon emissions. Traditional synthesis methods often rely on toxic chemicals, contributing to pollution and waste. In contrast, the green synthesis of ZnONPs leverages renewable biological materials, thereby decreasing reliance on synthetic reagents and reducing the overall carbon footprint associated with nanoparticle production.

Moreover, the biocompatibility and antimicrobial efficacy of these green-synthesized ZnONPs enhance their applicability in wound healing, potentially reducing the need for conventional antibiotics and their environmental implications.

Table 8 Effect of S. Obvallata ZnONPs on Wound Diameter, Wound Area and Percentage Wound Contraction

Groups	Wound Diameter (mm)						Area (mm sq)						Percentage Wound Contraction (%)					
	D0	D4	D8	D12	D16	D21	D0	D4	D8	D12	D16	D21	D0	D4	D8	D12	D16	D21
Excision (Control)	25.7 ± 0.5	24.5 ± 0.577	21.2 ± 0.829	15 ± 0.816	11.2 ± 0.957	7.25 ± 0.957	520.6 ± 20.01	471.3 ± 22.2	355.01 ± 31.6	177.01 ± 19.2	99.8 ± 16.6	41.8 ± 10.5	0	9.4 ± 3.5	31.6 ± 7.8	66.05 ± 2.7	80.8 ± 2.6	91.9 ± 2.2
ZnONPs	25.5 ± 0.577	23.25 ± 0.957	20 ± 0.707	10 ± 0.816	6.75 ± 0.957	3.75 ± 0.957	510.6 ± 23.1	424.8 ± 34.6	314.3 ± 25.6	78.8 ± 12.8	36.3 ± 10.4	11.5 ± 5.9	0	16.5 ± 8.5	38.4 ± 3.6	84.5 ± 2.4***	92.8 ± 2.2***	97.7 ± 1.2***
STD (Povidone-Iodine)	25 ± 0.577	23.25 ± 0.957	20 ± 0.707	9.25 ± 0.957	5.75 ± 0.957	0	510.6 ± 23.1	424.8 ± 34.6	314.3 ± 25.6	67.7 ± 13.6	26.4 ± 8.9	0	0	16.5 ± 8.5	38.3 ± 5.9	86.7 ± 2.6***	94.7 ± 1.9***	100***

Notes: Values are expressed as Mean±SEM for 6 animals per group. ***P<0.001 compared with controls (ANOVA followed by post-hoc tests for multiple comparisons).

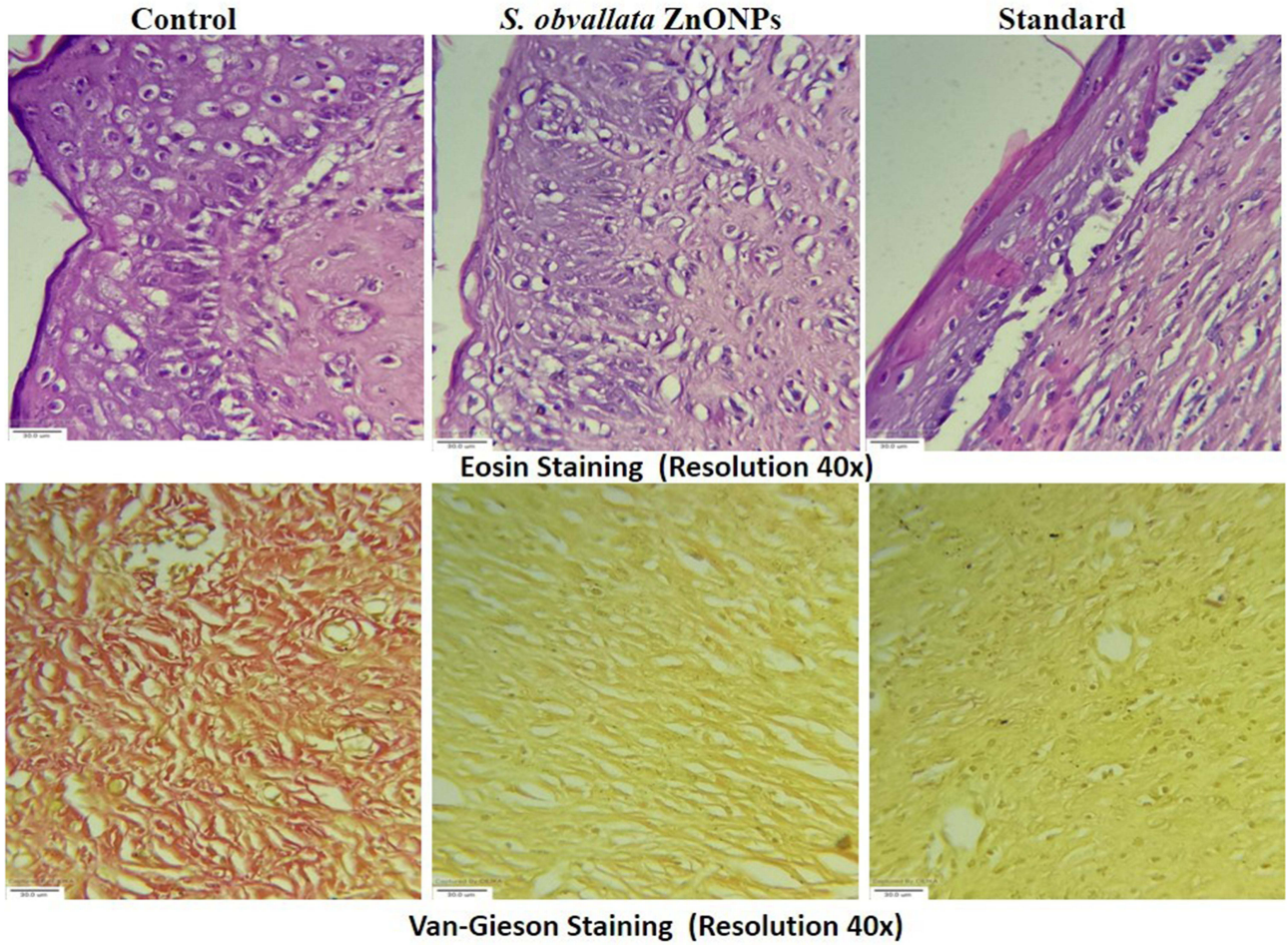

Figure 16 Histopathology images of newly regenerated tissue at day 21 (magnification 40X).

As healthcare increasingly prioritizes sustainability, the integration of such eco-friendly materials can lead to improved health outcomes while supporting broader sustainability goals.[64]

Conclusions

In the current research, the green synthesis of ZnONPs utilizing an aqueous extract of *S. obvallata* was investigated. The characterization revealed ZnONPs had an average size of 28 nm. The ZnONPs proved to be efficient against both gram-positive, gram-negative microorganisms and *C. albicans* fungal strain. The results of both in vitro and in vivo wound healing assays revealed the potent wound healing potential of the synthesized ZnONPs. The findings suggest that *S. obvallata* ZnONPs have the ability to effectively promote wound healing processes. Overall, the findings highlight the potential of *S. obvallata*-derived ZnONPs as a promising therapeutic agent for wound healing and infection management, while also underscoring the importance of sustainable and biocompatible approaches in the development of nanomaterials. Further research is warranted to explore the mechanisms of action and long-term safety of these nanoparticles in clinical applications.

Ethical Statement

The animal study protocol was reviewed and approved by the Najran University Scientific Research Ethical Committee (NUSREC), Najran, Saudi Arabia. The study was conducted in accordance with the local legislation prescribed by NUSREC and the National Committee of Bioethics, Saudi Arabia, and institutional requirements.

Acknowledgments

The authors extend their appreciation to the Deanship of Scientific Research at King of Khalid University for funding this work through Small Groups Project under grant number RGP1/17/45. The authors thank Najran University and KLE Technological University for supporting this study.

Author Contributions

All authors made a significant contribution to the work reported, whether that is in the conception, study design, execution, acquisition of data, analysis and interpretation, or in all these areas; took part in drafting, revising or critically reviewing the article; gave final approval of the version to be published; have agreed on the journal to which the article has been submitted; and agree to be accountable for all aspects of the work.

Disclosure

The authors declare that they have no known competing interests in this paper.

References

1. Guo Z-H, Khattak S, Rauf MA, et al. Role of Nanomedicine-Based Therapeutics in the Treatment of CNS Disorders. *Molecules*. 2023;28(3):1283. doi:10.3390/molecules28031283
2. Zheng Y, Cai X, Chen G, et al. Single Atom-Dispersed Silver Incorporated in ZIF-8-Derived Porous Carbon for Enhanced Photothermal Activity and Antibacterial Activities. *Int J Nanomed*. 2024;19:4253–4261. doi:10.2147/IJN.S459176
3. Laurent S, Forge D, Port M, et al. Magnetic Iron Oxide Nanoparticles: synthesis, Stabilization, Vectorization, Physicochemical Characterizations, and Biological Applications. *Chem Rev*. 2010;110:2574. doi:10.1021/cr900197g
4. Banfield JF, Zhang H. Nanoparticles in the Environment. *Rev Miner Geochem*. 2001;44:1–58. doi:10.2138/rmg.2001.44.01
5. Sastry M, Ahmad A, Islam Khan M, Kumar R. Biosynthesis of Metal Nanoparticles Using Fungi and Actinomycete. *Current Science*. 2003;85:162–170.
6. Rao MD, Gautam P. Synthesis and Characterization of ZnO Nanoflowers Using Chlamydomonas Reinhardtii: a Green Approach. *Environ Prog Sustainable Energy*. 2016;2016:1–7.
7. Ito A, Shinkai M, Honda H, Kobayashi T. Medical Application of Functionalized Magnetic Nanoparticles. *J Biosci Bioeng*. 2005;100:1–11. doi:10.1263/jbb.100.1
8. Fakhari S, Jamzad M, Kabiri Fard H. Green Synthesis of Zinc Oxide Nanoparticles: a Comparison. *Green Chem Lett Rev*. 2019;12:19–24. doi:10.1080/17518253.2018.1547925
9. Ac M, B R. Effect of Zinc Oxide Nanoparticles on Mechanical Properties of Diglycidyl Ether of Bisphenol-A. *J Mater Sci Eng*. 2016;5:291. doi:10.4172/2169-0022.1000291
10. Kalpana VN, Devi Rajeswari V. A Review on Green Synthesis, Biomedical Applications, and Toxicity Studies of ZnO NPs. *Bioinorg Chem Appl*. 2018;2018:1–12. doi:10.1155/2018/3569758
11. Bala N, Saha S, Chakraborty M, et al. Green Synthesis of ZnO NPs Using Hibiscus subdariffa Leaf Extract: effect of Temperature on Synthesis, Anti-Bacterial Activity and Anti-Diabetic Activity. *RSC Adv*. 2015;5:4993–5003. doi:10.1039/C4RA12784F
12. Kumar B, Smita K, Cumbal L, Debut A. Green Approach for Fabrication and Applications of Zinc Oxide Nanoparticles. *Bioinorg Chem Appl*. 2014;2014:523869. doi:10.1155/2014/523869
13. Supraja N, Prasad TNVKV, Krishna TG. Synthesis, Characterization, and Evaluation of the Antimicrobial Efficacy of Boswellia Ovalifoliolata Stem Bark-Extract-Mediated Zinc Oxide Nanoparticles. *Appl Nanosci*. 2016;6:581–590. doi:10.1007/s13204-015-0472-0
14. Khattak S, Xu H-T, Shen J. The microneedle bandages provide new hope for healing diabetic wounds. *Acta Pharmaceutica Sinica B*. 2024;14:5085–5087. doi:10.1016/j.apsb.2024.07.010
15. Asuncion E, Dimapilis S, Hsu C-S, Marie R, Mendoza O, Lu M-C. Zinc Oxide Nanoparticles for Water Disinfection. *Sustainable Environ Res*. 2018;28:47–56. doi:10.1016/j.serj.2017.10.001
16. Ginjupalli K, Alla R, Shaw T, Tellapragada C, Kumar Gupta L, Nagaraja Upadhya P. Comparative Evaluation of Efficacy of Zinc Oxide and Copper Oxide Nanoparticles as Antimicrobial Additives in Alginate Impression Materials. *Mater Today*. 2018;5:16258–16266. doi:10.1016/j.matpr.2018.05.117
17. Khatami M, Alijani HQ, Heli H, Sharifi I. Rectangular Shaped Zinc Oxide Nanoparticles: green Synthesis by Stevia and Its Biomedical Efficiency. *Ceram Int*. 2018;44:15596–15602. doi:10.1016/j.ceramint.2018.05.224
18. Lee K, Baek D-H, Na H, Choi J, Kim J. Simple Fabrication Method of Silicon/Tungsten Oxide Nanowires Heterojunction for NO2 Gas Sensors. *Sens Actuators B Chem*. 2018;265:522–528. doi:10.1016/j.snb.2018.03.100
19. Jaishi DR, Ojha I, Bhattarai G, et al. Plant-mediated synthesis of zinc oxide (ZnO) nanoparticles using Alnus nepalensis D. Don for biological applications. *Heliyon*. 2024;10(20):e39255. doi:10.1016/j.heliyon.2024.e39255
20. Iqbal J, Abbasi BA, Mahmood T, Kanwal S, Ahmad R, Ashraf M. Plant-Extract Mediated Green Approach for the Synthesis of ZnONPs: characterization and Evaluation of Cytotoxic, Antimicrobial and Antioxidant Potentials. *J Mol Struct*. 2019;1189:315–327. doi:10.1016/j.molstruc.2019.04.060
21. Semwal P, Painuli S. Antioxidant, Antimicrobial, and GC-MS Profiling of Saussurea obvallata (Brahma Kamal) from Uttarakhand Himalaya. *Clin Phytoscience*. 2019;5. doi:10.1186/s40816-019-0105-3
22. Şengönül H, Demircan O. Utilization of Prunus serrulata leaf extract for the synthesis and characterization of ZnO nanoparticles. *Nano-Struct Nano-Objects*. 2024;37:101084. doi:10.1016/j.nanoso.2023.101084

23. Nguyen DTC, Nguyen NTT, Nguyen TTT, Tran TV. Recent advances in the biosynthesis of ZnO nanoparticles using floral waste extract for water treatment, agriculture and biomedical engineering. *Nanoscale Adv*. 2024;6(16):4047–4061. PMID: 39114141; PMCID: PMC11302053. doi:10.1039/d4na00133h.
24. Xiang Y, Pan Z, Qi X. A cuttlefish ink nanoparticle-reinforced biopolymer hydrogel with robust adhesive and immunomodulatory features for treating oral ulcers in diabetes. *Bioact Mater*. 2024;39:562–581. doi:10.1016/j.bioactmat.2024.04.022
25. Singh V, Singh Y, Koirala R, Keshwa K, Tamta P, Singh TR. Therapeutic and cultural evaluation of Brahma Kamal (Saussurea obvallata (Dc.) Edgew: an endangered potential herb. *J Ayurveda Integrat Med Sci*. 2023;8(6):109–118. doi:10.21760/jaims.8.6.19
26. Ghosh D. Brahma Kamal: the Himalayan beauty. *Resonance*. 2017;22(4):377–387. doi:10.1007/s12045-017-0477-y
27. Sahu M, Sahu K, Sahu P, et al. Saussurea obvallata has its significance role in the treatment of wound healing: a review. *IJPS*. 2024. doi:10.5281/ZENODO.11097954
28. Kumar J, Pundir M. Phytochemistry and pharmacology of Saussurea genus (Saussurea lappa, Saussurea costus, Saussurea obvallata, Saussurea involucrata). *Mater Today Proc*. 2022;56:1173–1181. doi:10.1016/j.matpr.2021.11.145
29. Shilpakar A. *Phytochemical Screening and Analysis of Antibacterial and Antioxidant Activity of Ficus Auriculata, Lour*. Pokhara, Nepal: Stem Bark; 2009.
30. De S, Dey YN, Ghosh AK. Phytochemical Investigation and Chromatographic Evaluation of the Different Extracts of Tuber of Amorphaphallus paeoniifolius (Araceae). *Int J Pharm Biol Res*. 2010;1:150–157.
31. Paterson Phytochemical Methods. A Guide to Modern Techniques of Plant Analysis: j. B. Harborne. 15 × 23.4 Cm, 302 Pp. London: chapman & Hall, 1988. Price £79. ISBN 0-412-57260 (Hardback). *Plant Pathol*. 1999;48:146. doi:10.1046/j.1365-3059.1999.00318.x
32. Parekh J, Chanda S. In Vitro Antimicrobial Activity and Phytochemical Analysis of Some Indian Medicinal Plants. *Turk J Biol*. 2007;31:53–58.
33. Edeoga HO, Okwu DE, Mbaebie BO. Phytochemical Constituents of Some Nigerian Medicinal Plants. *Afr J Biotechnol*. 2005;4:685–688. doi:10.5897/ajb2005.000-3127
34. Mace ME, Bell AA, Beckman CH. Histochemistry and Identification of Disease-Induced Terpenoid Aldehydes in Verticillium-Wilt-Resistant and-Susceptible Cottons. *Can J Bot*. 1976;54:2095–2099. doi:10.1139/b76-225
35. Kumar P, Praveen S, Kumaravel C. Screening of Antioxidant Activity, Total Phenolics and GC-MS Study of Vitex Negundo. *Afr J Biochem Res*. 2010;4:191–195.
36. Onwukaeme DN, Ikuegbvweha TB, Asonye CC. Evaluation of Phytochemical Constituents, Antibacterial Activities and Effect of Exudate of Pycanthus Angolensis Weld Warb (Myristicaceae) on Corneal Ulcers in Rabbits. *Trop J Pharm Res*. 2007;6:725–730. doi:10.4314/tjpr.v6i2.14652
37. Dahiru D, Onubiyi JA, Umaru HA. Phytochemical Screening and Antiulcerogenic Effect of *Moringa Oleifera* AqueousLeaf Extract. *Afr J Tradit Complement Altern Med*. 2006;3. doi:10.4314/ajtcam.v3i3.31167.
38. Koczkur KM, Mourdikoudis S, Polavarapu L, Skrabalak SE. Polyvinylpyrrolidone (PVP) in Nanoparticle Synthesis. *Dalton Trans*. 2015;44:17883–17905. doi:10.1039/c5dt02964c
39. Anandalakshmi K, Venugobal J, Ramasamy V. Characterization of Silver Nanoparticles by Green Synthesis Method Using Pedalium Murex Leaf Extract and Their Antibacterial Activity. *Appl Nanosci*. 2016;6:399–408. doi:10.1007/s13204-015-0449-z
40. Taha R, Shojaei S. Fabrication, Functionalization, and Dispersion of Carbon Nanotubes. *Emerg Appl Nanopart Architect Nanostruct*. 2018;2018:501–531.
41. Eid MM. Characterization of Nanoparticles by FTIR and FTIR-Microscopy. In: *Handbook of Consumer Nanoproducts*. Singapore: Singapore; 2021:1–30.
42. Mansour H. *How to Analyze Nanoparticles Using EDS in the SEM?* Oxford Instruments; 2022.
43. Fultz B, Howe J. *Diffraction and the X-Ray Powder Diffractometer. Transmission Electron Microscopy and Diffractometry of Materials*. Springer; 2013.
44. Horváth G, Bencsik T, Ács K, Kocsis B. Sensitivity of ESBL-Producing Gram-Negative Bacteria to Essential Oils, Plant Extracts, and Their Isolated Compounds. *Antibiot Resist*. 2015;2015:239–269.
45. Balouiri M, Sadiki M, Ibnsouda SK. Methods for in Vitro Evaluating Antimicrobial Activity: a Review. *J Pharm Anal*. 2016;6:71–79. doi:10.1016/j.jpha.2015.11.005
46. Shaikh IA, Turakani B, Mahnashi MH, et al. Environmentally Friendly Production, Characterization, and Evaluation of ZnO NPs from Bixa Orellana Leaf Extract and Assessment of Its Antimicrobial Activity. *J King Saud Univ Sci*. 2023;35:102957. doi:10.1016/j.jksus.2023.102957
47. Muddapur UM, Turakani B, Jalal NA, et al. Phytochemical Screening of Bixa Orellana and Preliminary Antidiabetic, Antibacterial, Antifibrinolytic, Anthelmintic, Antioxidant, and Cytotoxic Activity against Lung Cancer (A549) Cell Lines. *J King Saud Univ Sci*. 2023;35:102683. doi:10.1016/j.jksus.2023.102683
48. Al Awadh AA, Shet AR, Patil LR, et al. Sustainable Synthesis and Characterization of Zinc Oxide Nanoparticles Using Raphanus Sativus Extract and Its Biomedical Applications. *Crystals*. 2022;12:1142. doi:10.3390/cryst12081142
49. Fronza MG, Baldinotti R, Martins MC, et al. Rational Design, Cognition and Neuropathology Evaluation of QTC-4-MeOBnE in a Streptozotocin-Induced Mouse Model of Sporadic Alzheimer's Disease. *Sci Rep*. 2019;9. doi:10.1038/s41598-019-43532-9
50. Woessner Jr JF. The Determination of Hydroxyproline in Tissue and Protein Samples Containing Small Proportions of This Imino Acid. *Arch Biochem Biophys*. 1961;93:440–447. doi:10.1016/0003-9861(61)90291-0
51. Haverkamp RG, Marshall AT. The Mechanism of Metal Nanoparticle Formation in Plants: limits on Accumulation. *J Nanopart Res*. 2009;11:1453–1463. doi:10.1007/s11051-008-9533-6
52. Jia C, Wu F-G. Antibacterial Chemodynamic Therapy: materials and Strategies. *BME Front*. 2023;4:0021. doi:10.34133/bmef.0021
53. Kaushik M, Niranjan R, Thangam R, et al. Investigations on the Antimicrobial Activity and Wound Healing Potential of ZnO Nanoparticles. *Appl Surf Sci*. 2019;479:1169–1177. doi:10.1016/j.apsusc.2019.02.189
54. Tong X, Lu J, Zhang W, et al. Efficacy and safety of external tissue expansion technique in the treatment of soft tissue defects: a systematic review and meta-analysis of outcomes and complication rates. *Burns Trauma*. 2022;10:tkac045. doi:10.1093/burnst/tkac045
55. Feng L, Liu Y, Xiang Q, et al. Injectable Antibacterial Hydrogel with Asiaticoside-Loaded Liposomes and Ultrafine Silver Nanosilver Particles Promotes Healing of Burn-Infected Wounds. *Adv Healthc Mater*. 2023;12:e2203201. doi:10.1002/adhm.202203201
56. Han G, Nguyen LN, Macherla C, et al. Nitric oxide-releasing nanoparticles accelerate wound healing by promoting fibroblast migration and collagen deposition. *Am J Pathol*. 2012;180(4):1465–1473. PMID: 22306734. doi:10.1016/j.ajpath.2011.12.013.

57. Alsareii SA, Manaa Alamri A, AlAsmari MY, et al. Synthesis and Characterization of Silver Nanoparticles from Rhizophora Apiculata and Studies on Their Wound Healing, Antioxidant, Anti-Inflammatory, and Cytotoxic Activity. *Molecules*. 2022;27:6306. doi:10.3390/molecules27196306
58. Mathew-Steiner SS, Roy S, Sen CK. Collagen in Wound Healing. *Bioengineering*. 2021;8:63. doi:10.3390/bioengineering8050063
59. Nahari MH, Al Ali A, Asiri A, et al. Green Synthesis and Characterization of Iron Nanoparticles Synthesized from Aqueous Leaf Extract of Vitex Leucoxylon and Its Biomedical Applications. *Nanomaterials*. 2022;12:2404. doi:10.3390/nano12142404
60. Augustine R, Nikolopoulos VK, Camci-Unal G. Hydrogel-Impregnated Self-Oxygenating Electrospun Scaffolds for Bone Tissue Engineering. *Bioengineering*. 2023;10:854. doi:10.3390/bioengineering10070854
61. Raza Ur Rehman S, Ullah A, Augustine R, et al. Enhanced wound healing by nanoengineered hydrogel patch loaded with connective tissue growth factor. *Mater Today Commun*. 2024;40(109825):109825. doi:10.1016/j.mtcomm.2024.109825
62. Huang Y, Bai L, Yang Y, Yin Z, Guo B. Biodegradable gelatin/silver nanoparticle composite cryogel with excellent antibacterial and antibiofilm activity and hemostasis for Pseudomonas aeruginosa-infected burn wound healing. *J Colloid Interface Sci*. 2022;608:2278–2289. doi:10.1016/j.jcis.2021.10.131
63. Metzke R Here's how healthcare can reduce its carbon footprint. World Economic Forum; 2022.Available from: https://www.weforum.org/stories/2022/10/cop27-how-healthcare-can-reduce-carbon-footprint/. Accessed November 30, 2024.
64. Kharissova AB, Kharissova OV, Kharisov BI, et al. Carbon Negative Footprint Materials: a Review. *Nano-Struct Nano-Objects*. 2024;37(101100):101100. doi:10.1016/j.nanoso.2024.101100